Sensorless Control of PM Motor Drives - a Technology Status Review

R. Bojoi, *Senior Member, IEEE*, M. Pastorelli, *Member, IEEE,* J. Bottomley, *Member, IEEE,* P. Giangrande, *Member, IEEE,* and C. Gerada, *Member, IEEE*

***Abstract*-- The control of Brushless Permanent Magnet Motors require rotor position information that can be measured by means of a position sensor. The motion sensorless control aims at eliminating the motor position sensor and its corresponding electronic conditioning circuits, cabling and connectors. Besides a clear cost reduction, the motion sensorless drives have better reliability when compared with their position sensor-based counterparts. The research conducted in the last two decades has provided many different solutions that are used in many applications. Nevertheless, the literature reports just a few survey papers dealing with this important topic. This paper intends providing a comprehensive review of the sensorless control solutions, including the machine influence on the sensorless drive performance.**

***Index Terms*—synchronous machines, brushless permanent magnet machines, sensorless control, back-electromotive force, observers, carrier signal injection, motor design.**

I. Introduction

THE control of brushless Permanent Magnet (PM) motors requires rotor position information that can be measured by means of position sensors, such as resolvers and encoders. The position sensors are expensive and very sensitive to mechanical stress, increasing the drive cost while reducing the overall reliability for drives operating in harsh environments. In addition, a position sensor requires special electronic condition circuitry, especially when the motor is far away respect to the controller system. In the past, the main application of PM motors was represented by the servodrives for machine tools and high performance positioning systems, where the additional cost involved by a high quality position sensor is fully justified.

Due to their high torque density and higher efficiency respect to other motor types, the PM motors have shown a continuous expanding in the Adjustable Speed Drives (ASDs) market to save energy in new domains as traction and automotive applications, electrical mobility, compressors, more electric aircraft, renewable power generation and home appliances. However, these applications often require high drive reliability, the motor is operated in harsh environment conditions with/or important cost limitations, such as in home appliances. For this reason, the elimination of the position sensor for these applications using sensorless control results in improved drive reliability and cost reduction [1-15].

The motion sensorless control aims at eliminating the position sensor and its corresponding electronic conditioning. Therefore, the rotor position must be obtained using only measured electrical quantities (such as motor currents, inverter DC link voltage, voltage at motor terminals, etc). Even if the position sensor is not completely removed, (such as in automotive and traction applications), the sensorless control is still used to provide a back-up rotor position information in case of position sensor failure.

The research work conducted in the last two decades in the field of sensorless control of PM motor drives has provided many different solutions that are today used in many applications. Nevertheless, the literature reports just a few survey papers dealing with sensorless control of PM motor drives [16,17].

The paper intends providing a comprehensive review of the sensorless control solutions, including the machine influence on the sensorless drive performance. The paper starts with an overview of the PM motor solutions and a classification of the sensorless control methods, together with the definition of the magnetic model of a PM machine. Then, a review of the sensorless control methods is performed. The paper ends with an analysis of PM motors capability for sensorless operation and how the motor design should be optimized to get best results, using a case study of an inset PM motor.

II. PM Motors and Classification of Sensorless Control Methods

The PM motor characteristics directly influence the choice of the sensorless control technique and also its performance. Therefore, a brief presentation of the different PM motor solutions is performed and a general classification of sensorless control methods is introduced.

A. Motor Design Solutions

The most used PM motor design solutions are shown in Fig.1.

R. Bojoi and M. Pastorelli are with Dipartimento Energia, Politecnico di Torino, Italy (e-mail: radu.bojoi@polito.it, michele.pastorelli@polito.it)

J. Bottomley, P. Giangrande and C. Gerada are with the PEMC group, University of Nottingham, UK, (e-mail: Chris.Gerada@nottingham.ac.uk)

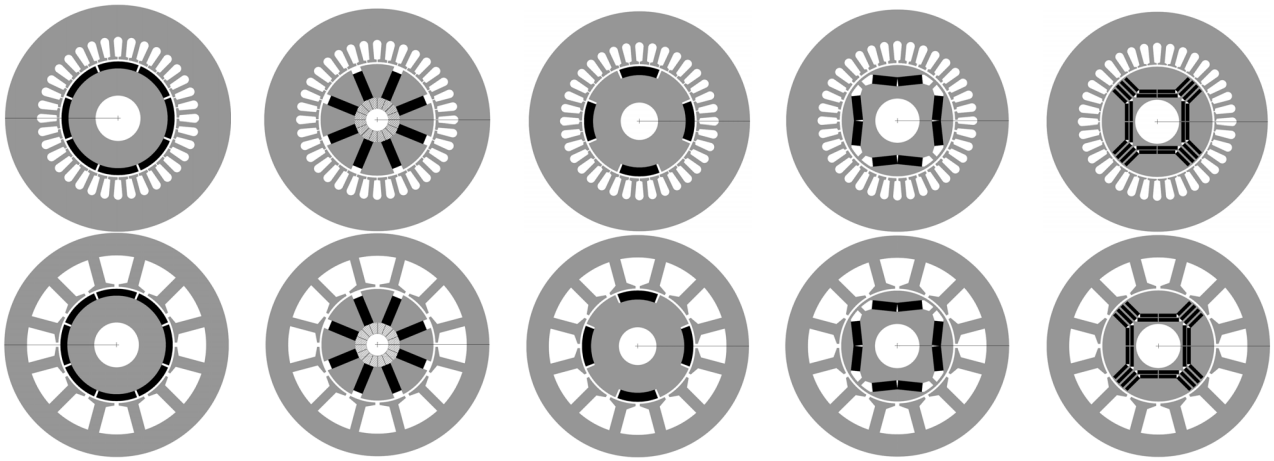

(a) SM PM motor (b) Flux-concentrating PM motor (c) Inset PM motor (d) Single layer IPM motor (e) Multi-layer IPM motor

Fig. 1. Cross sections of most used PM brushless motors, showing stator and rotor laminations (grey), PMs (black), stator slots (white) that contain distributed windings (top) or concentrated windings (bottom).

The stator can use distributed (overlapped) windings in a number of slots per pole and per phase higher or equal than unity, or concentrated windings placed in a number of slots per pole and per phase less than unity. The motors using the latter solution are also called fractional-slot PM motors.

The stator that uses concentrated windings is cheaper respect to the distributed windings solution, being very attractive in home appliances. Moreover, the motors with concentrated windings exhibit fault-tolerance operation, welcome in aerospace and traction applications and allows obtaining high pole pairs number, as required by direct motors drives requiring low speed and high torque.

The PM motor name is defined by the rotor structure. The Surface Mount (SM) rotor (Fig.1a) uses surface mounted magnets and represents a non-salient magnetic structure. The other rotor solutions are designed to achieve magnetic anisotropy by using buried magnets. The flux concentrating rotor (Fig.1b) and the inset PM rotor (Fig.1c) yield a moderate magnetic anisotropy, while the Internal PM (IPM) rotor (Fig.1d and Fig.1e) is characterized by high magnetic anisotropy, as high as the number of internal layers (or flux barriers) increases. The multiple-layer IPM motors are also known as PM-Assisted Synchronous Reluctance (PMASR) motors.

The magnetic saliency can be exploited for sensorless control, as will be shown later. However, a proper modeling approach is necessary to study the motor suitability for sensorless control. The modeling approach is based on the motor magnetic model described in the next section.

B. PM motors Magnetic Model

The magnetic model is the current-to-flux linkage relationship. The magnetic model is usually defined in rotating (d,q) rotor frame, where the d-axis is usually defined by the magnets north-pole, as shown in Fig.2 for SM PM motor and IPM motor. In case of PMASR motors, the d-axis is defined as the axis of minimum reluctance, as also shown in Fig.2. The difference between the two reference frames definition is just a phase shift of 90 electrical degrees. Using the SM PM (d,q) reference frame definition, the magnetic model of a PM machine is

$$\begin{bmatrix} \lambda_d \\ \lambda_q \end{bmatrix} = \begin{bmatrix} L_d & L_{dq} \\ L_{qd} & L_q \end{bmatrix} \cdot \begin{bmatrix} i_d \\ i_q \end{bmatrix} + \begin{bmatrix} \lambda_m \\ 0 \end{bmatrix} \tag{1}$$

where: L_d is the d-axis inductance, L_q is the q-axis inductance, $L_{dq} = L_{qd}$ are the cross-coupling inductances, λ_m is the magnets flux contribution.

The PM machines anisotropy is characterized by the so called anisotropy factor, defined as the ratio L_q/L_d. All inductances from (1) are apparent inductances.

According to their rotor structure, SM PM motors should exhibit no magnetic anisotropy and no cross-saturation, i.e. $L_d=L_q=L_s$ and $L_{dq}=L_{qd}=0$. However, the saturated SM PM motors may have an anisotropy induced by the magnetic saturation with cross-saturation depending by the machine operating point [18]. The flux-concentrating PM, the inset PM and IPM motors exhibit magnetic anisotropy, saturation and cross-saturation effects [19-22]. The PM motor magnetic model can be obtained from Finite Element Analysis (FEA) or from experimental identification, as in [23]. An example of a magnetic model of a three-layer IPM motor is shown in Fig.3.

With reference to the magnetic model (1), the average and difference inductances are defined as

$$L_{avg} = \frac{L_d + L_q}{2}, \; L_\Delta = \frac{L_q - L_d}{2} \tag{2}$$

Besides the rotor and stator design, the PM motors can subsequently divided into sinusoidal brushless PM motors and trapezoidal brushless PM motors. In the first case, the induced motional back-emf voltage in the stator windings is sinusoidal or near sinusoidal with low harmonic content and consequently the machine currents will be sinusoidal.

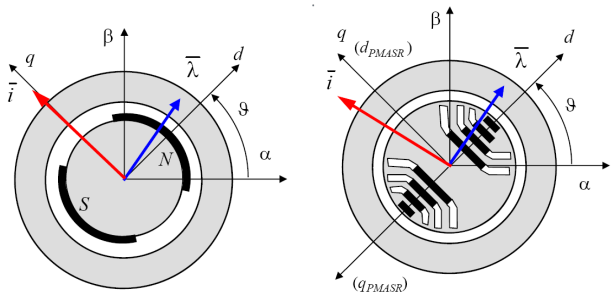

Fig. 2. Definition of (*d*,*q*) rotor frame based on the conventional definition for the SM PM motor and the PMASR motor

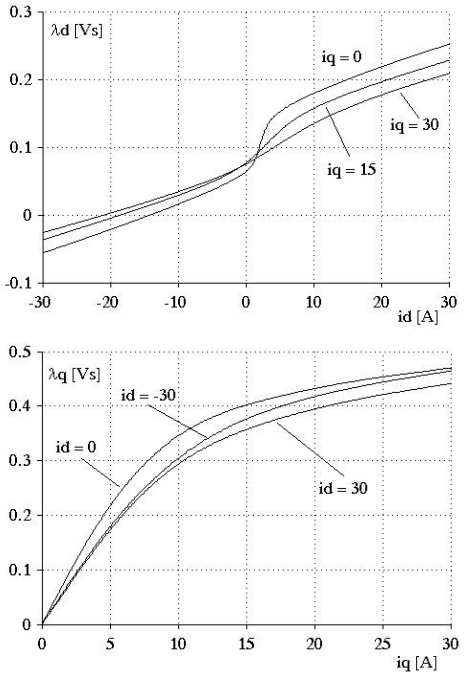

Fig. 3. Magnetic model of a three-layer IPM

The motors belonging to the second category have trapezoidal induced motional back-emf voltages and the phase currents are rectangular. As the sensorless control methods for trapezoidal PM motors have been covered in [15], *this paper focuses mainly on sinusoidal or near sinusoidal brushless PM machines and their sensorless control.*

C. Classification of Sensorless Control Methods

A classification of main sensorless control methods for brushless PM motors, with references from literature, is shown in Fig. 4. According to this classification, the sensorless control methods for brushless PM motors can be divided into two main categories:

- Methods based on excitation signals at fundamental motor frequency
- Methods based on excitation signals whose frequency is higher that the fundamental frequency

For both methods the PM motor magnetic modeling plays a key role in obtaining the desired performance.

III. Sensorless Methods Using Fundamental Excitation Signals

These methods use the machine model only for motor operation with excitation signals at fundamental frequency. The PM machine voltage model in phase coordinates is

$$[v]_{abc} = R_s \cdot [i]_{abc} + \frac{d}{dt}[\lambda]_{abc} \tag{3}$$

where: $[v]_{abc} = [v_a \quad v_b \quad v_c]^T$, $[i]_{abc} = [i_a \quad i_b \quad i_c]^T$, $[\lambda]_{abc} = [\lambda_a \quad \lambda_b \quad \lambda_c]^T$ are the voltage, the current and flux linkage vectors defined in phase coordinates.

The magnetic model in phase coordinates of a generic sinewound PM machine, considering only the fundamental field, is

$$[\lambda]_{abc} = \begin{bmatrix} L_{aa} & L_{ab} & L_{ac} \\ L_{ba} & L_{bb} & L_{bc} \\ L_{ca} & L_{cb} & L_{cc} \end{bmatrix} \cdot [i]_{abc} + \lambda_m \cdot \begin{bmatrix} cos\,\vartheta \\ cos(\vartheta - 2\pi/3) \\ cos(\vartheta + 2\pi/3) \end{bmatrix} \tag{4}$$

where:
$$L_{aa}(\vartheta) = L_{ls} + L_{g0} + L_{g2}\,cos(2\vartheta)$$
$$L_{bb}(\vartheta) = L_{ls} + L_{g0} + L_{g2} \cdot cos\,2(\vartheta - 2\pi/3)$$
$$L_{cc}(\vartheta) = L_{ls} + L_{g0} + L_{g2} \cdot cos\,2(\vartheta + 2\pi/3)$$
$$L_{ab}(\vartheta) = L_{ba} = -(1/2)L_{g0} + L_{g2} \cdot cos\,2(\vartheta - 2\pi/3)$$
$$L_{bc}(\vartheta) = L_{cb} = -(1/2)L_{g0} + L_{g2} \cdot cos\,2(\vartheta)$$
$$L_{ca}(\vartheta) = L_{ac} = -(1/2)L_{g0} + L_{g2} \cdot cos\,2(\vartheta + 2\pi/3)$$

L_{ls} is the leakage inductance, L_{g0} and L_{g2} are inductances corresponding to the magnetic field at the airgap

Using the not power invariant Clarke transformation, the machine voltage model in stationary (α,β) frame is

$$\bar{v}_{\alpha\beta} = R_s \cdot \bar{i}_{\alpha\beta} + \frac{d\bar{\lambda}_{\alpha\beta}}{dt} \tag{5}$$

where: $\bar{v}_{\alpha\beta} = v_\alpha + jv_\beta$, $\bar{i}_{\alpha\beta} = i_\alpha + ji_\beta$ and $\bar{\lambda}_{\alpha\beta} = \lambda_\alpha + j\lambda_\beta$ are the voltage, current and flux vectors defined in the (α,β) stationary reference frame (Fig.2).

The machine magnetic model in stationary frame is

$$\begin{bmatrix} \lambda_\alpha \\ \lambda_\beta \end{bmatrix} = \begin{bmatrix} L_{avg} + L_\Delta\,cos(2\vartheta) & L_\Delta\,sin(2\vartheta) \\ L_\Delta\,sin(2\vartheta) & L_{avg} - L_\Delta\,cos(2\vartheta) \end{bmatrix} \cdot \begin{bmatrix} i_\alpha \\ i_\beta \end{bmatrix} + \begin{bmatrix} \lambda_{m\alpha} \\ \lambda_{m\beta} \end{bmatrix} \tag{6}$$

where: $\lambda_{m\alpha} = \lambda_m\,cos(\vartheta)$, $\lambda_{m\beta} = \lambda_m\,sin(\vartheta)$, $L_\Delta = (3/2)L_{g2}$ and $L_{avg} = L_{ls} + (3/2)L_{g0}$ and.

The machine voltage equations in (*d*,*q*) rotor frame is

$$\bar{v}_{dq} = R_s \cdot \bar{i}_{dq} + \frac{d}{dt}\bar{\lambda}_{dq} + j \cdot \omega \cdot \bar{\lambda}_{dq} \tag{7}$$

where the magnetic model in (*d*,*q*) frame is given in (1).

Most fundamental excitation methods have been applied to non-salient PM motors. In this case, the rotor position and speed information is contained by the motional back-emf voltages and also by the phase inductances in case of saturated PM machines.

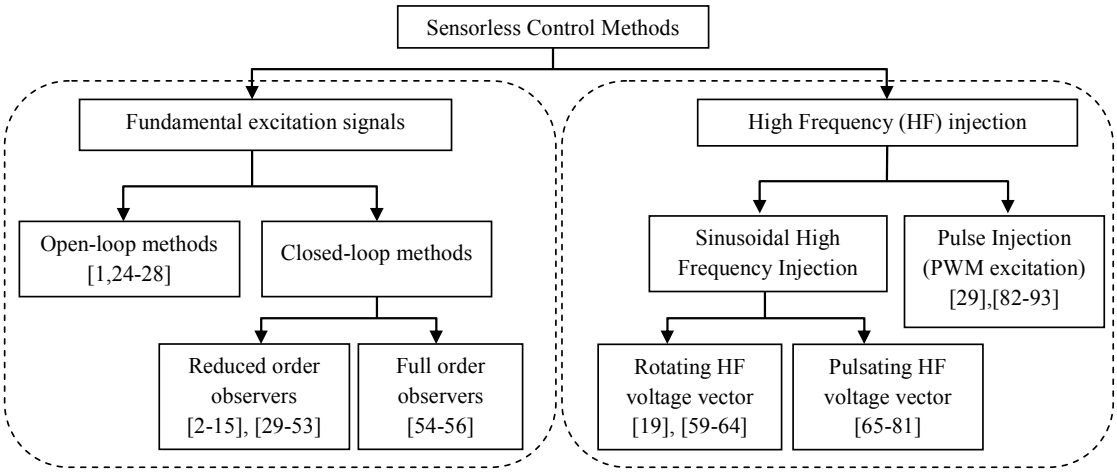

Fig. 4. Classification of sensorless control methods for brushless PM motors with reference to literature

A. Open-Loop Methods

The open-loop methods obtain the rotor position information from the machine model and from direct sensing of the motor voltage terminals, without using an internal correction mechanism.

The direct sensing of motor terminal voltages [1,24] is very popular for brushless DC machines used in appliances, where the voltage of the non-conducting phase contains information about both rotor position and speed. This method gives good results when the required starting torque is very low and no zero speed operation is required. Another solution that uses direct voltage sensing to exploit the third harmonic voltages, that are synchronized with the rotor, is described in [25].

Direct sensing of line-to-line voltages was used in [26,27] for an SM PM motor and a flux-concentrating PM motor, to get the machine flux linkage using the stator voltage integration. This solution is very simple but with strong limitations regarding the minimum frequency and also the starting torque capability, being thus suitable for pumps and fans [26]. The solution from [26] used vector control in flux coordinates, while the solution adopted in [27] used vector control with the rotor position estimated from the stator flux position and an estimation of the load angle.

Another solution is to use the motional back-emf voltages from the machine model, as in [28]. This method is implemented in a rotating frame whose position error, respect to the real rotor frame, is obtained using a simplified voltage model at constant currents. This method is very sensitive to the inverter dead-time effects and resistance variation. The reported minimum speed operating value at rated load conditions was 50 rpm [28].

B. Closed-Loop Methods

In contrast with the open-loop methods, the closed-loop techniques are based on observer schemes that use an internal correction mechanism, as shown in Fig.5. Most observers use the Model Reference Adaptive System (MRAS) approach that is shown in Fig. 5.

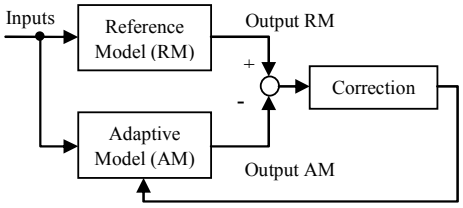

Fig. 5. Generic closed-loop observer

A simplified classification of the closed-loop methods includes the reduced-order observers and full-order observers.

C. Reduced-Order Observers

The reduced-order observers are closed-loop schemes that do not contain the mechanical motor model. From the literature, the most employed reduced-order observer schemes are depicted in Figs. 6-8. The voltage, current and flux vectors can be referred to any reference frame, i.e., phase coordinates, stationary (α,β) frame or rotating frame.

1) Reduced-order current observers

For these observers (Fig.6), the reference model is the motor whose outputs are the currents, while the adaptive model is the motor model that estimates the motor currents. The error between the estimated currents and the measured ones is fed back to the adaptive model. The rotor position is obtained according to the adopted reference frame.

An observer with the adaptive model implemented in rotating frame is presented in [29] for a SM PM machine. In this case, the algorithm does not estimate the absolute rotor position, but the incremental position between two sampling periods. This scheme needs initial rotor position that was obtained using a pulse injection method. The minimum speed at load conditions was 35 rpm for a 6-poles machine.

Another solution is to implement the current observer in the stationary frame. In this case, the observer provides the absolute rotor position by estimating the motional back-emf voltages

$$\begin{cases} \hat{e}_\alpha = -\hat{\omega}\cdot\lambda_m\cdot sin(\hat{\vartheta}) \\ \hat{e}_\beta = \hat{\omega}\cdot\lambda_m\cdot cos(\hat{\vartheta}) \end{cases} \Rightarrow \hat{\vartheta} = tan^{-1}\left(-\frac{\hat{e}_\alpha}{\hat{e}_\beta}\right) \quad (8)$$

Obviously, this solution cannot work at zero speed since the back-emf voltages are zero.

The solution presented in [30] for an IPM motor employed a reduced-order Kalman filter whose state variables are the stator currents and the motional back-emf voltages. A different observer implementation can use the sliding mode approach, as in [31], where the correction mechanism gets first the rotor speed, then the rotor position is obtained by integrating the estimated speed. A minimum speed of 50 rpm for an 8 poles SM PM motor has been obtained. Other sliding mode current observers have been also implemented in [10,32].

A current observer with minimization of the speed estimation error using the instantaneous reactive power was presented in [33] for an 8 poles SM PM motor. The minimum speed at 35% rated load conditions was 50 rpm.

In case of IPM motors with high anisotropy factor, the use of reduced-order observers needs a particular attention, due to the different inductances on (d,q) axes.

By neglecting the cross-saturation, the magnetic model (1) can be also written as (9).

$$\begin{cases} \lambda_d = L_d\cdot i_d + \lambda_m = L_q\cdot i_d + \lambda_m + (L_d - L_q)\cdot i_d \\ \lambda_q = L_q\cdot i_q = L_d\cdot i_q - (L_d - L_q)\cdot i_q \end{cases} \quad (9)$$

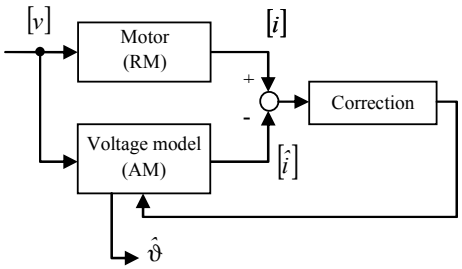

Fig. 6. Reduced-order current observer

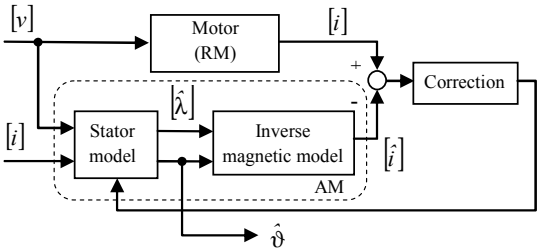

Fig. 7. Reduced-order current observer with inverse magnetic model

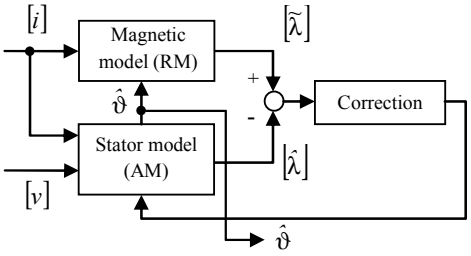

Fig. 8. Reduced-order flux observer

Using (9), the voltage model in rotor frame (7) becomes [34-36]:

$$\begin{bmatrix} v_d \\ v_q \end{bmatrix} = \begin{bmatrix} R_s + pL_d & -\omega L_q \\ \omega L_q & R_s + pL_d \end{bmatrix}\cdot\begin{bmatrix} i_d \\ i_q \end{bmatrix} + \begin{bmatrix} 0 \\ E_{sal} \end{bmatrix} \quad (10)$$

where: $p = d/dt$ is the derivative operator

$E_{sal} = \omega\cdot[\lambda_m + (L_d - L_q)] - (L_d - L_q)\cdot\frac{d}{dt}i_q$ was called extended back-emf voltage in rotor frame [34-36].

The voltage model (10) can be easily transformed in (α,β) stationary reference frame as

$$\begin{bmatrix} v_\alpha \\ v_\beta \end{bmatrix} = \begin{bmatrix} R_s + pL_d & -\omega(L_d - L_q) \\ \omega(L_d - L_q) & R_s + pL_d \end{bmatrix}\cdot\begin{bmatrix} i_\alpha \\ i_\beta \end{bmatrix} + E_{sal}\cdot\begin{bmatrix} -sin\vartheta \\ cos\vartheta \end{bmatrix} \quad (11)$$

As shown in (11), the extended back-emf voltage components contain information on the rotor position and can be used for PM motors with saliency.

The papers [34-36] implemented a reduced-order observer using the extended back-emf concept to estimate the rotor position. While [34] has been implemented in rotor frame, [35,36] have been implemented in stationary reference frame. The solution presented in [35] used an observer whose state variables were the currents and the extended back-voltage components, [36] used a simpler linear observer having only the currents as state variables. In this case, the extended back emf voltages are extracted directly from the correction mechanism, after a proper decoupling of the terms depending on the motor saliency. To filter the position calculated with (8), a position observer with torque feedforward has been also proposed in [36].

Based on the extended back-emf concept, other solutions have been proposed. A sliding mode current observer was proposed in [37], while an enhanced current-rotor flux observer was employed in [38].

An enhanced current-rotor flux observer implemented in stationary reference frame was proposed in [39] for a SM PM motor. Besides the adaptive speed estimation, this solution includes also an adaptive stator resistance adaptation mechanism only for low speed operation. The experimental results showed a minimum speed of 20 rpm for 6 poles motor at load conditions.

A nonlinear current and back-emf reduced order observer was proposed in [40,41] for PM motors with arbitrary back-emf waveforms. The minimum speed at load conditions that has been used during the experimental tests was 100 rpm for a 16-poles, axial flux PM machine with non-sinusoidal back emf waveform.

A sensorless method the d-axis output of the current controller is presented in [2],[42] for high speed PM motor drives. Although this method does not use a true current observer, it can be considered as a closed-loop method due to the closed-loop current control.

2) Reduced-order current observers with inverse magnetic model

For these observers (Fig.7), the reference model is the motor whose outputs are the currents, while the adaptive model consists of the voltage model and the inverse magnetic model. The flux components are estimated first, then the currents are computed suing the inverse magnetic model. The error between the estimated currents and the measured ones is fed back to the adaptive model to correct the estimated flux components.

Reduced-order observers with inverse magnetic model implemented in phase coordinates are presented in [43-45] for both trapezoidal and sinusoidal SM PM motors. The flux-to-current relationship is very complex since it is obtained as the inverse model of (4).

The sensorless methods from [46] and [47] are based on reduced-order observers implemented in (α,β) frame for two different IPM motors. The reported minimum frequency for [46] was 3 Hz, while the minimum speed at rated load reported in [47] was 30 rpm for a 6 poles motor.

The solution presented in [48] is an adaptive current observer with inverse magnetic model implemented in an estimated rotor reference frame. The error between the measured and the estimated currents is used also for speed estimation; the rotor position is obtained by speed integration. As the minimum operating speed was found as 0.02 pu, the solution from [48] was combined with a HF injection for very low speed operation.

Although similar as concept, a different solution was presented in [49,50] for IPM motors, where the rotor position was provided by the machine flux using the "active flux" (or extended flux) approach [52] described in the next subsection. A stator resistance estimation algorithm was also proposed. Using an accurate inverse magnetic model and also a proper compensation of the inverter dead-time effects, [49,50] reported zero speed operation with load transients.

3) Reduced-Order Flux Observers

For these observers (Fig.8), the reference model is the magnetic model whose inputs are the motor currents and the rotor position, while the adaptive model consists of the voltage model. The error between the outputs of the two models is fed back to correct the stator voltage integration. The flux observer may be particularly interesting when a Direct Torque Control (DTC) scheme is adopted for the PM machine since the DTC directly regulates the flux and torque.

The flux observer needs the rotor position. One solution may use high frequency injection at low speed, while at high speed a simple integration can be employed [51].

Another alternative is getting the rotor position from the voltage model using the "active flux concept" [52] that has been introduced for PM motors with saliency. By neglecting the cross-saturation, the magnetic model (1) is modified as

$$\begin{bmatrix}\lambda_d\\ \lambda_q\end{bmatrix}=\begin{bmatrix}L_q & 0\\ 0 & L_q\end{bmatrix}\cdot\begin{bmatrix}i_d\\ i_q\end{bmatrix}+\begin{bmatrix}\lambda_a\\ 0\end{bmatrix} \tag{12}$$

where $\lambda_a=\lambda_m+\left(L_d-L_q\right)\cdot i_d$ is the magnitude of the "active flux" vector whose position is the rotor position.

The inverse magnetic model of (12) in rotating frame is extremely simple [49,50]:

$$\begin{bmatrix}i_d\\ i_q\end{bmatrix}=\begin{bmatrix}L_q^{-1} & 0\\ 0 & L_q^{-1}\end{bmatrix}\cdot\begin{bmatrix}\lambda_d-\lambda_a\\ \lambda_q\end{bmatrix} \tag{13}$$

The magnetic model (12) can be easily transformed in stationary reference frame as

$$\begin{bmatrix}\lambda_\alpha\\ \lambda_\beta\end{bmatrix}=\begin{bmatrix}L_q & 0\\ 0 & L_q\end{bmatrix}\cdot\begin{bmatrix}i_\alpha\\ i_\beta\end{bmatrix}+\begin{bmatrix}\lambda_{a,}\cdot cos\vartheta\\ \lambda_{a,}\cdot sin\vartheta\end{bmatrix} \tag{14}$$

The "active flux" concept allows considering an IPM motor as a PM machine with no saliency [52]. The active flux components components contain information on the rotor position. The active flux components in stationary frame are estimated from the estimated flux components and the rotor position is computed as

$$\begin{bmatrix}\hat{\lambda}_{a,\alpha}\\ \hat{\lambda}_{a,\beta}\end{bmatrix}=\begin{bmatrix}\hat{\lambda}_\alpha-L_q\cdot i_\alpha\\ \hat{\lambda}_\beta-L_q\cdot i_\beta\end{bmatrix}\Rightarrow\hat{\vartheta}=tan^{-1}\left(\frac{\hat{\lambda}_\alpha}{\hat{\lambda}_\beta}\right) \tag{14}$$

Flux observers using (14) and the magnetic model were proposed in [53,54] for a single-layer IPM motor. The minimum speed at rated load conditions was 2 rpm (0.1 Hz). The same approach has been used in [23] for direct-drive SM PM motors for horizontal-axis washers, showing good starting capability from zero speed with torque overload capability up to two times rated torque and with wide speed range operation (maximum speed is four times the base speed).

As happens for the above presented reduced-order solution, the flux observers need the initial rotor position and their performance depend on the magnetic model accuracy, the stator resistance and the inverter dead-time effects.

D. Full-Order Observers

For these observers (Fig.9), the reference model is the motor whose outputs are the currents, while the adaptive model is the motor model that estimates the motor currents. Respect to previous observers, the full-order observers include the mechanical model whose output is the rotor position that is used to get the estimated currents via the inverse magnetic model. The error between the estimated currents and the measured ones is fed back to the adaptive model.

A first attempt of full-order observer was proposed in [54] for a SM PM motor, showing a particular sensitivity with mechanical parameter detuning, such as inertia and the load torque. As consequence, an adaptation of mechanical parameters had to be implemented, with a lot of limitations due to the reduced computational resources.

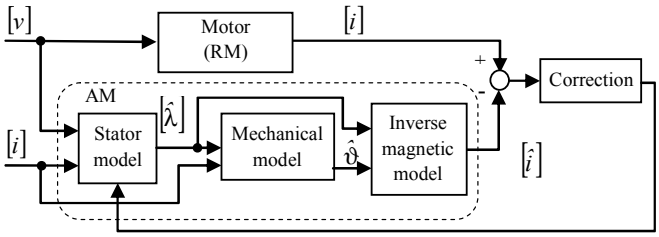

Fig. 9. Full-order observer with mechanical model

The full-order observer solution that provided better results is the Extended Kalman Filter (EKF) proposed in [55,56]. The EKF uses as state variables the stator current components in stationary reference frame, the rotor speed and the rotor position. The EKF is more robust to mechanical parameter detuning, but the provided experimental results showed rather poor performance at very low speed operation due to inverter dead-time effects and measurement issues.

E. Comments on Sensorless Methods Using Fundamental Excitation Signals

The literature reports many sensorless methods using fundamental excitation signals. Final comments regarding these methods are briefly summarized as follows:

- The methods cannot work well below a certain minimum speed, depending on the adopted scheme.
- The performance at low speed is significantly improved when using accurate magnetic models, proper inverter dead-time compensation schemes, adaptation of parameters (i.e. stator resistance), accurate current and voltage acquisition [57].
- The initial position is required, so initial position detection schemes must be included in the overall algorithm. Sometimes, with low starting torques, the detection of the initial position can be avoided or the rotor can be aligned to a fixed position imposed by a stator current vector.
- For wide speed range applications that require also zero speed operation, the fundamental frequency sensorless method must be combined with a sensorless method based on high frequency injection in a hybrid solution [51,58].

IV. SENSORLESS CONTROL METHODS WITH HIGH FREQUENCY INJECTION

For these methods, special High Frequency (HF) signals are superimposed on the excitation signals of fundamental frequency to exploit the PM machine saliency mainly given by the rotor anisotropy. While the fundamental frequency quantities are involved in the electromechanical energy conversion, the high frequency signals allow exploiting the machine saliencies for rotor position detection. With reference to the magnetic model (1) defined in (*d,q*) rotor frame, high frequency injection means small variations around a certain operating point in the (*d,q*) plane. The magnetic model for HF injection becomes [19-22]

$$\begin{bmatrix}\lambda_{dh}\\ \lambda_{qh}\end{bmatrix}=\begin{bmatrix}L_{dh} & L_{dqh}\\ L_{qdh} & L_{qh}\end{bmatrix}\cdot\begin{bmatrix}i_{dh}\\ i_{qh}\end{bmatrix} \tag{15}$$

where L_{dh}, L_{qh}, $L_{dqh} = L_{qdh}$ *are differential inductances* corresponding to the operating point in the (*d,q*) plane.

The average and difference inductances corresponding to the differential inductances are

$$L_{avgh}=\frac{L_{dh}+L_{qh}}{2},\ L_{\Delta h}=\frac{L_{qh}-L_{dh}}{2} \tag{16}$$

By using the complex notation and introducing the complex conjugate current vector $\bar{i}_{hf}^{*}=i_{dh}-ji_{qh}$, the HF magnetic model (15) becomes [19]

$$\bar{\lambda}_{dqh}=L_{avgh}\cdot\bar{i}_{dqh}+\left(L_{\Delta h}+j\cdot L_{dqh}\right)\cdot\bar{i}_{dqh}^{*} \tag{17}$$

In (17) are clearly emphasized the contributions of positive and negative sequence current components. In addition, because of the cross-saturation inductance L_{dqh}, the negative sequence current component is rotated by an angle

$$\varepsilon=tan^{-1}\frac{L_{dq}}{L_{\Delta h}} \tag{18}$$

The HF inverse magnetic model flux-to-current is obtained from (17) as

$$\bar{i}_{dqh}=\frac{L_{avg}}{\Delta}\bar{\lambda}_{dqh}-\left(\frac{L_{\Delta h}}{\Delta}+j\cdot\frac{L_{dqh}}{\Delta}\right)\cdot\bar{\lambda}_{dqh}^{*} \tag{19}$$

where $\Delta=\begin{vmatrix}L_{dh} & L_{dqh}\\ L_{dqh} & L_{qh}\end{vmatrix}=L_{dh}\cdot L_{qh}-L_{dqh}^{2}$.

Most HF injection methods inject voltages (flux) using two main approaches (Fig.4). The first one employs a continuous injection with sinusoidal signals, while the second one applies discontinuous voltages (or voltage pulses).

A. Sinusoidal High Frequency Injection Methods

When a sinusoidal HF voltage is superimposed on the fundamental voltage, sinusoidal HF currents appear in the motor windings, according to the HF motor model. The HF currents contain information related to the rotor position that must be extracted by the sensorless method by means of a proper demodulation scheme. It is assumed that the injected frequency is much higher than the fundamental frequency.

The literature reports two injection techniques that are briefly summarized as follows.

1) Rotating voltage vector (revolving carrier)

In this case, a voltage vector at constant carrier frequency ω_h is superimposed on the reference voltages produced by the machine control in stationary reference frame

$$\bar{v}_{\alpha\beta h}=V_h\cdot e^{j(\omega_h t)}=V_h\cdot\left[cos(\omega_h t)+j\,sin(\omega_h t)\right] \tag{20}$$

By neglecting the stator resistance, the corresponding HF current vector is the sum of a positive and negative sequence HF components described as

$$\bar{i}_{\alpha\beta h} = \bar{i}_{\alpha\beta h,p} + \bar{i}_{\alpha\beta h,n}$$
$$\bar{i}_{\alpha\beta h,p} = \frac{L_{avgh}}{\Delta} \cdot \frac{\bar{v}_{\alpha\beta h}}{j\omega_h} \quad (21)$$
$$\bar{i}_{\alpha\beta h,n} = -\left(\frac{L_{\Delta h}}{\Delta} + j\frac{L_{dqh}}{\Delta} \right) \cdot e^{j2\vartheta} \cdot \frac{\bar{v}^*_{\alpha\beta h}}{j\omega_h}$$

From (21) it can be seen that the negative sequence HF current component contains information related to the rotor position. If the negative sequence component is extracted by a demodulation system, then the angle (2ϑ) can be obtained. However, the cross-saturation will produce an error on the estimated rotor position; it was shown in [19] that this position error is equal to $\varepsilon/2$ since the angle $(2\vartheta+\varepsilon)$ is tracked by the demodulation process.

The HF method with rotating voltage vector was proposed in [59] for salient AC motors, including induction machines having a rotor saliency caused by the spatial modulation of the rotor leakage inductance. A closed-loop position and speed tracking scheme, consisted of a heterodyning demodulator and a Luenberger position observer with estimated feedforward torque, has been proposed. Although the paper focused mainly on the induction machine, the authors suggested that the AC machines should be purposely designed for sensorless operation using high frequency injection. The solution introduced in [59] was also applied in [60] for a single-layer IPM motor.

The HF injection with rotating voltage vector has been used for multi-layer IPM motors in [19,21,62] and also for inset PM motors in [21].

A simple HF injection technique was proposed in [61] for a flux concentrating PM motor. Instead of using a continuous position tracking through a closed-loop scheme, this solution simply detects the zero-crossings, the positive and the negative peaks of the negative sequence current component. As a result, the rotor position is "sampled" with a frequency that is 4 times the injected frequency.

A modified HF rotating vector method is proposed in [63] for an IPM motor drive. Instead of using a constant amplitude HF voltage, a speed varying amplitude is used, producing an ellipse trajectory for the injected HF voltage vector. A new PLL tracking scheme has been proposed.

The literature reports a rather limited popularity of the HF injection with rotating voltage vector for PM machines [21,59-64]; this technique is more popular for induction motor drives [17,64].

2) Pulsating voltage vector (alternating carrier)

In this case, a pulsating voltage vector is superimposed on an estimated *d*-axis voltage component at constant carrier frequency ω_h, i.e.

$$v_{dh} = V_h \cdot cos(\omega_h t)$$
$$v_{qh} = 0 \quad (22)$$

Using a similar procedure as for the previous injection method, the corresponding HF current vector components in the estimated $(\hat{d},\hat{q})$ rotor reference frame

$$\tilde{i}_{dh} = \frac{V_h}{\omega_h} \cdot \left[\frac{L_{avgh}}{\Delta} + \frac{L_{\Delta h}}{\Delta} cos(2\vartheta_{err}) - \frac{L_{dqh}}{\Delta} sin(2\vartheta_{err}) \right] sin(\omega_h t)$$
$$\tilde{i}_{qh} = \frac{V_h}{\omega_h} \cdot \left[\frac{L_{\Delta h}}{\Delta} sin(2\vartheta_{err}) + \frac{L_{dqh}}{\Delta} cos(2\vartheta_{err}) \right] sin(\omega_h t) \quad (23)$$

where $\vartheta_{err} = \vartheta - \hat{\vartheta}$ is the angle error between the estimated $(\hat{d},\hat{q})$ and the real (d,q) rotor frame.

Equation (23) shows that the amplitude of the *q*-axis HF current components contains information on the position error, so it must be extracted by the sensorless method. The *q*-axis HF component should be zero in case of perfect orientation. However, the cross-saturation will produce an error on the estimated rotor position, as happens with the rotating voltage vector injection.

The HF method with pulsating voltage vector was introduced in [65] for a single-layer IPM motor, using a similar heterodyning demodulator and a position closed-loop observer that were proposed in [59].

In contrast to the previous HF injection method, the HF injection with pulsating voltage vector is more employed [65-77]. The differences between the proposed solutions are related to: (1) the processing of the estimated *q*-axis current from (23) to properly detect the rotor position, (2) the PM motor used for the implementation and (3) the detection of the initial rotor position.

The analysis performed in [21] for a three-layer IPM and an inset PM demonstrated that the two sinusoidal HF injection methods obtain the same results. However, [67,68,73] suggested that the HF injection using pulsating voltage vector yields better results for PM SM motors, where the machine saliency is given by the magnetic saturation and not by the rotor anisotropy. Moreover, the resulting HF current does not produce torque, with a clear benefit in terms of noise and vibrations. The experimental results for [67,68,73] showed very good performance, especially when the demodulator is properly synchronized with the PWM modulation [73].

A completely different approach for SM PM motors has been proposed in [75,76]. This method exploits the eddy-current reflected asymmetric resistance for position estimation. In this case, the HF model takes into account the stator resistance, that exhibits different *d*-axis and *q*-axis values, due to the enhanced eddy-current produced by the frequency injection [75,76].

B. Pulse Injection (PWM Excitation)

For these methods, the rotor position is detected by injecting test voltage vectors on specified directions in stationary frame during very short time intervals. In case of an existing excitation at fundamental frequency, the test vector must be superimposed on the voltage vector rotating at fundamental frequency.

The *di/dt* of the phase currents, resulting from the application of the test vectors, are used to identify the differential phase inductance along the direction of the test vector. As the phase inductances are rotor position dependent, this information can be used to detect the rotor position at standstill or at low speed operation. However, a special attention must be dedicated to the PWM pattern in order to avoid current distortion due to the additional test vectors and the influence of the PWM switching and common mode capacitive currents.

A pulse injection method called "INFORM" was introduced in [82] and subsequently optimized in [83-85]. This method interrupts the PWM pattern to apply the test vectors and needs a particular measurement sequence of the phase currents, in order to detect properly the phase *di/dt*. The error in the rotor position was found in the range 3-15 electrical degrees.

A similar approach was used in [86] for an IPM motor, but without interrupting the PWM pattern. A special *di/dt* measurement technique, synchronized with the PWM pulses, and a dedicated hardware have been used. The experimental results reported a position error below 10 electrical degrees [86].

Other pulse injection methods [87,88] aimed at reducing the currents distortion using optimized PWM patterns or at increasing the speed range [89,90] for IPM motors.

The pulse injection can be successfully used for initial rotor position at standstill to initialize properly a sensorless method using either fundamental excitation or sinusoidal HF injection [29,91-93]. The peak currents corresponding to the voltage pulses are used to determine the d-axis rotor position with a reasonable accuracy that is enough to allow motor starting. The advantage of using these methods is that no particular measurement sequence and hardware is needed for initial position detection.

C. Comments on Sensorless Methods using Sinusoidal HF Injection

The literature reports different sensorless methods using sinusoidal HF injection. Final comments regarding these methods are briefly summarized as follows:

- The sinusoidal HF injection is an effective method for sensorless operation of all PM motors, including zero speed under load conditions
- The generation of the injected voltage (shape, frequency, magnitude), the inverter dead-time effects, the quality of the currents acquisition feedback and the filter selection strongly influence the performance of the rotor position tracking operation [17,73,78-81,113]
- The performance of the sensorless methods are strongly influenced by the machine magnetic model; in particular, the cross-saturation produces position estimation error that is load dependent [19-21]. For this reason, the experimental tuning of the HF injection method is often done using a trial-end-error approach, according to the used PM machine
- The magnetic model must be analysed to check if a suitable value the difference inductance $L_{\Delta h}$ exists for all operating points in the (d,q) plane
- For wide-speed range sensorless PM motor drives, the sinusoidal HF injection method should be employed only at low speed, while sensorless high speed operation is obtained by a sensorless method based on fundamental excitation signals

V. PM MOTOR SENSORLESS OPERATION CAPABILITY AND MOTOR DESIGN OPTIMIZATION

A. PM Motor Sensorless Capability

Sensorless control of PM machines has three distinct forms of operation, high speed detection, low/zero speed detection and initial position detection. The recent trend of hybrid control schemes [51,58] allows comprehensive control across the whole operational envelope, by utilizing motional back-emf voltage for high speed operation and HF injection for low/zero speed detection.

Therefore, a PM machine must exhibit various characteristics for sensorless capability. Firstly, a HF frequency saliency is needed, created by the differential inductances along the *d* and *q*-axis [20,21,94-97]. However, it is desirable to have a large saliency ratio to improve the signal-to-noise ratio and consequently to reduce the amplitude of the required injection signal.

The differential inductances are typically both position (Fig. 10) and load dependent (Fig. 11).

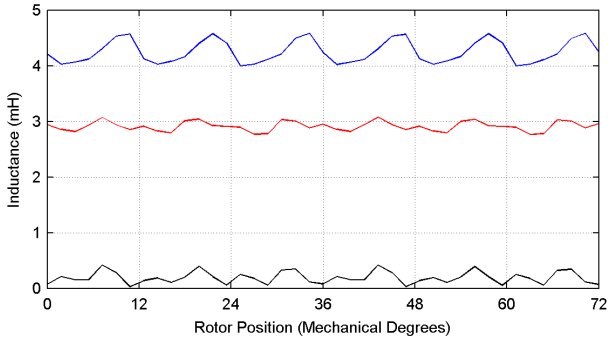

Fig. 10. HF differential inductance variation with rotor position: L_{dh} (red), L_{qh} (blue), L_{dqh} (black).

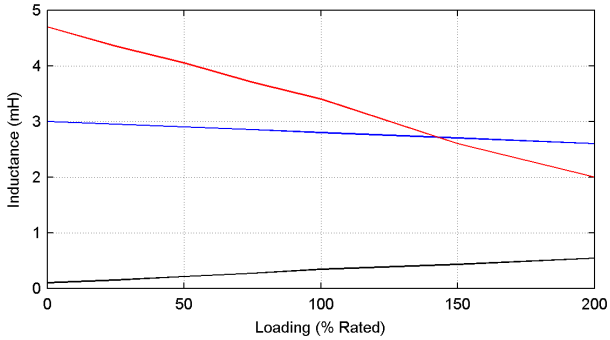

Fig. 11. HF differential inductance variation with motor load: L_{dh} (red), L_{qh} (blue), L_{dqh} (black).

In particular, the *q*-axis inductance saturates under increasing load, in many cases heavily. This characteristic can cause PM machines with HF saliency to have a unity saliency ratio at various points in the operational envelope. This is illustrated in Fig. 11, where L_{qh} saturates to the extent where it is equal to L_{dh} at around 150% rated load. At these locations where a zero saliency condition occurs, HF tracking control schemes will fail and therefore it is an important consideration when sensorless capability is a requirement. The potential impact of this condition is investigated by determining the HF saliency throughout the whole loading range to ensure zero saliency does not occur [20-22].

As already demonstrated in Chapter IV, another important aspect within the machine is the cross-saturation condition, causing an error in the estimated position. The cross-saturation within a PM machine is load dependent and therefore the angular offset increases with load. Compensation is often used within the sensorless control scheme to account for the load dependent phase shift. The compensation must be calculated however, commonly through commissioning tests with an encoder or FEA. Therefore, a low level of cross-saturation is advantageous, as it reduces the need for phase-shift compensation and position error [18,19,98-100]. Having said this, it is usually accepted that if the machine is designed to minimise it, it would significantly impact the fundamental torque producing capability of the machine.

B. Sensorless-Oriented PM Motor Design

The majority of research related to sensorless control of PM machines to date has focused on the control side of the problem. The remainder of work addresses the machine design, most importantly accounting for sensorless properties during topological design. As with all design processes, there must be a compromise between achieving a machine that can be controlled sensorlessly while maintaining a certain level of performance. Ultimately when concerned with sensorless oriented design, it is simplest to target the HF saliency characteristics.

The initial selection of machine structure influences the specific set of design challenges associated with sensorless properties. Most notably, there is a large increase in natural saliency when changing from an SPM structure to an IPM structure. While the use of distributed or concentrated windings influences saliency characteristics. The various advantages of each rotor design have been investigated over recent years [20,21,101]. Although the overall machine structure is likely to be selected solely based on the fundamental performance, there are specific challenges for each topology.

Sensorless orientated design generally focuses on the impact of variations to either the rotor or stator geometry. The research mostly investigates small variations to one or two geometrical parameters within a small region in an attempt to limit impact of overall performance. IPM machines offer a vast amount of design options, whether it is the size, shape and orientation of the PMs, flux barriers or several PMs per pole. With this comes a large amount of customisation with sensorless oriented design, [102-104] demonstrate a number of approaches to investigating the influence of IPM rotor geometry on sensorless capability. The expanded investigation from [104-106] uses a typical IPMSM design and optimizes it for various applications. The expansion of the feasibility region is one of the main design considerations, ensuring the machine can operate within the requirements. A variety of geometrical parameters are optimized, including embedding depth of PM, PM length and rotor tooth opening. A top down approach is used, where each parameter is set in a define sequence. This approach uses each parameter to improve a specific sensorless or performance characteristic. Here careful selection of the rotor tooth opening (θ_{rt}) and PM length (l_m) are used to increase the *q*-axis differential inductance and reduce the *d*-axis differential inductance. In [107] the authors design two distinct PM motors; the topologies aim to use flux intensifying IPMs (FIIPMSM) for improving sensorless performance. Analytical comparison carried out with a standard IPMSM topology. The unique designs improved the feasibility region by creating an inverse saliency characteristic ($L_q<L_d$), removing the possibility of a crossover point. In addition, careful design allows for reduced cross coupling and secondary saliencies.

Research into sensorless control of SM PM motors has been less common in the past due to the perception that IPM machines are more advantageous in the role. However, various works have been carried out and looked at sensorless oriented design [22,108,109].

Surface-mount and inset PM motors in general have a low natural saliency due to the limited variation in the *d*-axis and *q*-axis reluctance paths; this is a particular concern for the former. This increases the likelihood of zero saliency points within the operational envelope. In [108] the investigation is based on improving the signal-to-ratio ratio for the position tracking signals without compromising the overall performance. This is achieved through varying the slot/pole combination and using stator bridges across the slot opening. FEA analysis is used to investigate the impact of saturation on the saliency signals, along with the 6^{th} spatial harmonic within the inductance profile.

The possibly benefits of an inset rotor design over an IPM rotor design are discussed in [22]. Despite the IPM motor often being the preferred choice for zero speed sensorless control, the inset machine does have limited rotor saturation due to the large flux path. It is demonstrated how this can improve position estimation at high loads. Another benefit of this topology comes from the higher PM flux within the machine; this enables improved estimation during initial position detection. In general terms, varying geometrical parameters can be used to target improvements

in saliency characteristics. The data in Table I and Table II indicates how a machine topology can be optimized solely based on fundamental performance and to include sensorless characteristics.

TABLE I. MACHINE DESIGN PARAMETERS

	Initial Topology	Fundamental Optimization	Sensorless Optimization
Stack Length	87.6mm	87.6mm	87.6mm
Stator Outer Diameter	67.5mm	67.5mm	67.5mm
Split Ratio	0.6	0.558	0.558
Tooth Width	11mm	12mm	12mm
Back Iron Thickness	5mm	5.7mm	5.7mm
Magnet Span	36.5°	36°	36°
Slot Opening	7°	7°	7.7°
Tooth Tip	1.375mm	1.375mm	0.75mm
Tooth Bridge	3.5mm	3.5mm	2mm
Magnet Inset	50 %	50 %	30 %

The data is based on a simple 9-slots, 8-poles inset PM topology (Fig.12) and demonstrates how various parameters could influence the main saturation saliency of the machine. During this process, the main machine dimensions influencing the overall performance are used during the fundamental optimization.

TABLE II. PERFORMANCE ANALYSIS

	Initial Topology	Fundamental Optimization	Sensorless Optimization
Rated Torque	32.2 Nm	33.7 Nm	34 Nm
Torque Ripple	3.41 %	2.38 %	3.05 %
Saliency (at Rated)	0.80	0.87	1.09

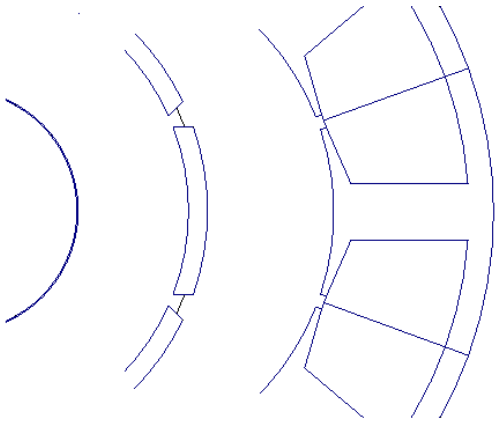

Fig. 12. Sketch of a 9-slots, 8-poles machine design topology.

As a progression, small variations are made to further geometrical parameters to improve the saliency characteristics with limited impact on the fundamental properties. The increase in saliency ratio, which shifts the zero saliency point to above rated load, comes at a cost as some of the improve torque ripple is lost. Although not targeted during this optimization stage it does however marginally increase the rate torque production.

The issue of L_q saturation under load causing a zero saliency condition is specifically addressed in [95]. The approach used involves designing an SPMSM topology that has an inverse saliency under all loading conditions. This essentially means with increasing load the saliency ratio will improve. The introduction of a zigzag flux (commonly found when concerned with induction machines) through careful parameter selection creates an increase in the q-axis reluctance path and therefore a reduction in the q-axis inductance. Inverse saliency is a simple solution to zero saliency points providing it can be achieved with limited impact on the machine performance.

The winding configuration, distributed or concentrated, affects the sensorless capability of PM machines. In [110] both forms are analysed with regards to three rotor configurations. Sensorless performance is based on the saliency ratio, level of cross-saturation and presence of secondary saliencies, over a large loading range. With these topologies, it is shown that concentrated windings can generate more saliency, however this is along with an increase in secondary saliencies which generally increase estimated position error.

A relatively new approach to sensorless oriented design is to account for certain sensorless machine characteristics during machine design optimization. The main objective here, in general, is still to focus on the fundamental machine performance while considering the sensorless ability of the machine, as in [111,112]. However, the optimization routine should ensure that there is no zero saliency condition within the entire operational envelope for motor.

VI. CONCLUSIONS

The sensorless control represents today an effective and mature technology for PM motor drives. From the analysis of the provided literature, it results that the knowledge of the motor magnetic model is a key issue in sensorless control, not only from the point of view of the rotor position tracking, but also to obtain the best motor exploitation for the application. The inverter non-linear effects, the quality of the current and voltage acquisition, the generation of the injected voltage (shape, frequency, magnitude) and the filter selection strongly influence the performance of the rotor position tracking.

The paper provides a review of the sensorless control solutions for PM motor drives, including the machine design influence on the sensorless drive performance. In addition, the paper includes also an analysis of PM motor capability for sensorless operation and how the motor design should be optimized to get best results. These

aspects are explained by means of a case study using an inset PM motor.

VII. REFERENCES

[1] K. Iizuka, H. Uzuhashi, M. Kano, T. Endo, and K. Mohri, "Microcomputer Control for Sensorless Brushless Motor,", *IEEE Tran. Ind. Applicat.*, vol. IA-21, no. 4, pp.595-601, May/June 1985.

[2] B.-H. Bae, S.-K. Sul, J.-H. Kwon, and J.-S. Byeon, "Implementation of Sensorless Vector Control for Super-High-Speed PMSM of Turbo-Compressor,", *IEEE Tran. Ind. Applicat.*, vol. 39, no. 3, pp. 811-818, May/June 2003.

[3] J.X. Shen, and K.J. Tseng, "Analyses and Compensation of Rotor Position Detection Error in Sensorless PM Brushless DC Motor Drives,", IEEE Tran. Energy Conv. , vol. 18, no.1, pp. 87-93, March 2003.

[4] M. Naidu, T.W. Nehl, S. Gopalakrishnan, and L Wurth, "A semi-integrated, sensorless PM brushless drive for a 42-V automotive HVAC compressor", *IEEE Ind. Applicat. Magazine*, pp. 20-28, July/August 2005.

[5] T.D. Batzel and K.Y. Lee, "Electric Propulsion With Sensorless Permanent Magnet Synchronous Motor: Implementation and Performance,", *IEEE Tran. Energy Conv.*, vol. 20, no.3, pp. 575-583, September 2005.

[6] J. Goetz, H. Weiping, and J. Milliken,"Sensorless digital motor controller for high reliability applications," Proc. of IEEE APEC Conf., March 2006.

[7] M. Morimoto, K. Aiba, T. Sakurai, A. Hoshino, and M. Fujiwara, "Position Sensorless Starting of Super High-Speed PM Generator for Micro Gas Turbine,", *IEEE Tran. Ind. Electron.*, vol. 53, no. 2, pp. 415-420, April 2006.

[8] T. Halkosaari, "Speed Sensorless Vector Control of a Redundant Permanent Magnet Wind Power Generator," Proc. of IEEE ISIE Conf. pp.2595-2600, June 2007.

[9] S.G. Burrow P.H. Mellor, P. Churn, T. Sawata, and M. Holme, "Sensorless Operation of a Permanent-Magnet Generator for Aircraft,", *IEEE Tran. Ind. Applicat.*, vol. 44, no. 1, pp. 101-107, January/February 2008.

[10] S. Chi, Z. Zhang, and L. Xu, "Sliding-Mode Sensorless Control of Direct-Drive PM Synchronous Motors for Washing Machine Applications,", *IEEE Tran. Ind. Applicat.*, vol. 45, no. 2, pp. 582-590, March/April 2009.

[11] M.-F. Hsieh and H.-J. Liao, "A wide speed range sensorless control technique of brushless dc motors for electric propulsors," *Journal of Marine Science and Technology*, vol. 18, no. 5, pp. 735-745, 2010.

[12] R. Bojoi, B. He, F. Rosa, and F. Pegoraro, "Sensorless Direct Flux and Torque Control for Direct Drive washing machine applications," *Proc. of IEEE ECCE*, pp.347-354, September 2011.

[13] F. Demmelmayr, M. Troyer, and M.Schroedl, "Advantages of PM-machines compared to induction machines in terms of efficiency and sensorless control in traction applications,", *Proc. of the IEEE IECON Conf.*, vol., no., pp.2762-2768, November 2011.

[14] F. Demmelmayr, M. Susic, and M. Schroedl, "Sensorless control at high starting torque of a 4000 Nm traction drive with permanent magnet synchronous machine," *Proc. of the EPE Conf.*, pp.1-8, 2011.

[15] W. Qiao, X. Yang, and X. Gong; , "Wind Speed and Rotor Position Sensorless Control for Direct-Drive PMG Wind Turbines," ,", *IEEE Tran. Ind. Applicat.*, vol. 48, no. 1, pp. 3-11, January/February 2012.

[16] P. Acarnley, and J.F. Watson, "Review of Position-Sensorless Operation of Brushless Permanent-Magnet Machines,", *IEEE Tran. Ind. Electron.*, vol. 53, no. 2, pp. 352-361 April 2006.

[17] F. Briz and M.W. Degner, "Rotor Position Estimation-A Review of High-Frequency Methods,", *IEEE Ind. Electron. Magazine*, pp. 24-36, June 2011.

[18] T. Frenzke, "Impact of cross-saturation on sensorless control of surface permanent magnet synchronous motors", *Conf . Rec. European Conference on Power Electronics and Applications EPE* 2005.

[19] P. Guglielmi, M. Pastorelli, and A. Vagati, "Cross-Saturation Effects in IPM Motors and Related Impact on Sensorless Control,", *IEEE Tran. Ind. Applicat.*, vol. 42, no. 6, pp. 1516-1522, November/December 2006.

[20] N. Bianchi, and S. Bolognani, "Influence of Rotor Geometry of an IPM Motor on Sensorless Control Feasibility,", *IEEE Tran. Ind. Applicat.*, vol. 43, no. 1, pp. 87-96, January/February 2007.

[21] N. Bianchi, S. Bolognani, J.-H. Jang and, S.-K. Sul, "Comparison of PM Motor Structures and Sensorless Control Techniques for Zero-Speed Rotor Position Detection,", *IEEE Tran. Power Electron.*, vol. 22, no. 6, pp. 2466-2475, November 2007.

[22] N. Bianchi, S. Bolognani, J.-H. Jang, and S.-K. Sul, "Advantages of Inset PM Machines for Zero-Speed Sensorless Position Detection,", *IEEE Tran. Ind. Applicat*., vol. 44, no. 4, pp. 1190-1198, July/August 2008.

[23] E. Armando, R. Bojoi, O. Guglielmi, G. Pellegrino, and M. Pastorelli, "Experimental methods for synchronous machines evaluation by an accurate magnetic model identification", *Conf. Rec. IEEE ECCE* 2011, pp. 1744-1749.

[24] H.-B. Wang, and H.-P. Liu, "A novel sensorless control method for brushless DC motor,", *IET Electric Power Applicat.*, vol. 3, iss. 3, pp.240-246, 2009.

[25] J.C. Moreira, "Indirect Sensing of Rotor Flux Position of Permanent Magnet AC Motors Operating Over a Wide Speed Range,", *IEEE Tran. Ind. Applicat.*, vol. 32, no. 6, pp. 1394-1401, November/December 1996.

[26] R.Wu, and G.S. Slemon, "A Permanent Magnet Motor Drive Without a Shaft Sensor", IEEE Tran. On Ind. Applicat., vol.27, no.5, September/October 1991, pp.1005-1011.

[27] A. Consoli, S. Musumeci, A. Raciti, and A. Testa, "Sensorless Vector and Speed Control of Brushless Motor Drives,", *IEEE Tran. Ind. Electron.*, vol. 41, no. 1, pp. 91-96, February 1994.

[28] J.-S. Kim and S.-K. Sul, "New Approach for High-Performance PMSM Drives Without Rotational Position Sensors,", *IEEE Tran. Power Electron.*, vol. 12, no. 5, pp. 904-911, September 1997.

[29] N. Matsui, "Sensorless PM Brushless DC Motor Drives,", *IEEE Tran. Ind. Electron.*, vol. 43, no. 2, pp. 300-308, April 1996.

[30] Y.-H. Kim and Y.-S. Kook, "High Performance IPMSM Drives without Rotational Position Sensors Using Reduced-Order EKF,", *IEEE Tran. Energy Conv.*, vol. 14, no.4, pp. 868-873, December 1999.

[31] Y.-S. Han, J.-S. Choi and, Y.-S- Kim, "Sensorless PMSM Drive with a Sliding Mode Control Based Adaptive Speed and Stator Resistance Estimator,", *IEEE Tran. Magn.*, vol. 36, no. 5, pp. 3588-3591, September 2000.

[32] Y. Liu, Z.Q. Zhu, and D. Howe, "Instantaneous Torque Estimation in Sensorless Direct-Torque-Controlled Brushless DC Motors,", *IEEE Tran. Ind. Applicat.*, vol. 42, no. 5, pp. 1275-1283, September/October 2006.

[33] Y.S. Kim, Y.K. Choi, and J.H. Lee, "Speed-sensorless vector control for permanent-magnet synchronous motors based on instantaneous reactive power in the wide-speed region," *IEE Pro.*, Vol. 152, No.5, pp. 1343-1349, September 2005.

[34] S. Morimoto, K. Kawamoto, M.Sanada, and Y. Takeda, "Sensorless Control Strategy for Salient-Pole PMSM Based on Extended EMF in Rotating Reference Frame,", *IEEE Tran. Ind. Applicat.*, vol. 38, no. 4, pp. 1054-1061, July/August 2002.

[35] Z. Chen, M. Tomita, S. Doki, and S. Okuma, "An Extended Electromotive Force Model for Sensorless Control of Interior Permanent-Magnet Synchronous Motors,", *IEEE Tran. Ind. Electron.*, vol. 50, no. 2, pp. 288-295, April 2003.

[36] H. Kim, M.C. Harke, and R.D. Lorenz, "Sensorless Control of Interior Permanent-Magnet Machine Drives With Zero-Phase Lag Position Estimation,", *IEEE Tran. Ind. Applicat.*, vol. 39, no. 6, pp. 1726-1733, November/December 2003.

[37] S. Sayeef, G. Foo and M.F. Rahman, "Rotor Position and Speed Estimation of a Variable Structure Direct-Torque-Controlled IPM Synchronous Motor Drive at Very Low Speeds Including Standstill,", *IEEE Tran. Ind. Electron.*, vol. 57, no. 11, pp. 3715-3723, November 2010.

[38] M. Hasegawa, S. Yoshioka, and K. Matsui, "Position Sensorless Control of Interior Permanent Magnet Synchronous Motors Using Unknown Input Observer for High Speed Drives,", *IEEE Tran. Ind. Applicat.*, vol. 45, no. 3, pp. 938-946, May/June 2009.

[39] M. Rashed, P.F.A. MacConnell, A. Fraser Stronach, and P. Acarnley "Sensorless Indirect-Rotor-Field-Orientation Speed Control of a Permanent-Magnet Synchronous Motor With Stator-Resistance

Estimation,", *IEEE Tran. Ind. Electron.*, vol. 54, no. 3, pp. 1664-1675, June 2007.
[40] C.H. De Angelo, G.R. Bossio, J.A. Solsona, G.O. Garcia and M.I. Valla, "Sensorless speed control of permanent-magnet motors with nonsinusoidal EMF waveform," *IEE Proc.-Electr. Power Appl.*, Vol. 152, No.5, pp. 1119-1126, September 2005.
[41] C. De Angelo, G. Bossio, J. Solsona , G.O. Garcia, and M.I. Valla, "Mechanical Sensorless Speed Control of Permanent-Magnet AC Motors Driving an Unknown Load,", *IEEE Tran. Ind. Electron.*, vol. 53, no. 2, pp. 406-414, April 2006.
[42] J.-K. Seok, J.-K. Lee, and D.-C. Lee, "Sensorless Speed Control of Nonsalient Permanent-Magnet Synchronous Motor Using Rotor-Position-Tracking PI Controller,", *IEEE Tran. Ind. Electron.*, vol. 53, no. 2, pp. 399-405, April 2006.
[43] N. Ertugrul and P. Acarnley, "A New Algorithm for Sensorless Operation of Permanent Magnet Motors,", *IEEE Tran. Ind. Applicat.*, vol. 30, no. 1, pp. 126-133, January/February 1994.
[44] C. French and P. Acarnley, "Control of Permanent Magnet Motor Drives Using a New Position Estimation Technique,", *IEEE Trans. Ind. Applicat.* ,vol. 32, no.5, pp. 1089-1097, September/October 1996.
[45] N. Ertugrul and P. Acarnley, "Indirect Rotor Position Sensing in Real Time for Brushless Permanent Magnet Motor Drives,", *IEEE Tran. Power Electron.*, vol. 13, no. 4, pp. 608-616, July 1998.
[46] S. Ostlund and M. Brokemper, "Sensorless Rotor-Position Detection from Zero to Rated Speed for and Integrated PM Synchronous Motor Drive,", *IEEE Tran. Ind. Applicat.*, vol. 32, no. 5, pp. 1158-1165, September/October 1996.
[47] S. Shinnaka, "New Sensorless Vector Control Using Minimum-Order Flux State Observer in a Stationary Reference Frame for Permanent-Magnet Synchronous Motors,", *IEEE Tran. Ind. Electron.*, vol. 53, no. 2, pp. 388-398, April 2006.
[48] A. Piippo, M. Hinkkanen, and J. Luomi, "Analysis of an Adaptive Observer for Sensorless Control of Interior Permanent Magnet Synchronous Motors,", *IEEE Tran. Ind. Electron.*, vol. 55, no. 2, pp. 570-576, February 2008.
[49] G. Foo and M.F. Rahman, "Sensorless vector control of interior permanent magnet synchronous motor drives at very low speed without signal injection,", *IET Electric Power Applicat.*, vol. 4, iss. 3, pp. 131-139, 2010.
[50] G. Foo and M.F. Rahman, "Sensorless Direct Torque and Flux-Controlled IPM Synchronous Motor Drive at Very Low Speed Without Signal Injection,", *IEEE Tran. Ind. Electron.*, vol. 57, no. 1, pp. 395-403, January 2010.
[51] Gh.-D. Andreescu, C.I. Pitic, F. Blaabjerg, and I. Boldea, "Combined Flux Observer With Signal Injection Enhancement for Wide Speed Range Sensorless Direct Torque Control of IPMSM Drives,", *IEEE Tran. Energy Conv.* , vol. 23, no.2, pp. 393-402, June 2008.
[52] I. Boldea, M.C. Paicu, Gh.-D. Andreescu, and F. Blaabjerg, "Active-Flux" DTFC-SVM Sensorless Control of IPMSM,", *IEEE Tran. Energy Conv.*, vol. 24, no. 2, pp. 314-1322, June 2009.
[53] M.C. Paicu, I. Boldea, G.D. Andreescu, and F. Blaabjerg, "Very low speed performance of active flux based sensorless control: interior permanent magnet synchronous motor vector control versus direct torque and flux control,", *IET Electric Power Applicat.*, vol. 3, iss. 6, pp.551-561, 2009.
[54] R. B. Sepe and J.H. Lang, "Real-Time Observer-Based (Adaptive) Control of a Permanent-Magnet Synchronous Motor without Mechanical Sensors,", *IEEE Tran. Ind. Applicat.*, vol. 28, no. 6, pp. 1345-1352, November/December 1992.
[55] S. Bolognani, R. Oboe, and M. Zigliotto, "Sensorless Full-Digital PMSM Drive With EKF Estimation of Speed and Rotor Position," *IEEE Tran. Ind. Electron*., vol. 46, no.1, pp.184-191, February 1999.
[56] S. Bolognani, L. Tubiana and M. Zigliotto, "EKF-Based Sensorless IPM Synchronous Motor Drive for Flux-Weakening Applications,", *IEEE Tran. Ind. Applicat.*, vol. 39, no. 3, pp. 768-775, May/June 2003.
[57] R.W. Hejny and R.D. Lorenz, "Evaluating the Practical Low-Speed Limits for Back-EMF Tracking-Based Sensorless Speed Control Using Drive Stiffness as a Key Metric,", *IEEE Tran. Ind. Applicat.*, vol. 47, no. 3, pp. 1337-1343, May/June 2011.
[58] C. Silva, G.M. Asher, and M. Sumner "Hybrid Rotor Position Observer for Wide Speed-Range Sensorless PM Motor Drives Including Zero Speed,", *IEEE Tran. Ind. Electron.*, vol. 53, no. 2, pp. 373-378, April 2006.
[59] P.L. Jansen, and R.D. Lorenz, "Transducerless position and velocity estimation in induction and salient AC machines", *IEEE Tran. Ind. Applicat.*, Vol.31, Issue 2, 1995, pp.240-247.
[60] L. Wang, and R.D. Lorenz, "Rotor position estimation for permanent magnet synchronous motor using saliency-tracking self-sensing method", *Conf. Rec. IEEE IAS* 2000, vol.1, pp. 445-450.
[61] A. Consoli, G. Scarcella, and A. Testa, "Industry Application of Zero-Speed Sensorless Control Techniques for PM Synchronous Motors,", *IEEE Tran. Ind. Applicat.*, vol. 37, no. 2, pp. 513-521, March/April 2001.
[62] P. Guglielmi, M. Pastorelli, G. Pellegrino, and A. Vagati, "Position-Sensorless Control of Permanent-Magnet-Assisted Synchronous Reluctance Motor,", *IEEE Tran. Ind. Applicat.*, vol. 40, no. 2, pp. 615-622, March/April 2004.
[63] S. Shinnaka, "A New Speed-Varying Ellipse Voltage Injection Method for Sensorless Drive of Permanent-Magnet Synchronous Motors With Pole Saliency—New PLL Method Using High-Frequency Current Component Multiplied Signal,", *IEEE Tran. Ind. Applicat.*, vol. 44, no. 3, pp. 777-788, May/June 2008.
[64] C.S. Staines, C. Caruana, N. Teske, J. Cilia, and G. Asher, "Sensorless speed, position and torque control using AC machine saliencies", *Proc. of IEEE ICIT Conf.* 2004, vol.1, pp.466-473.
[65] M.J. Corley and R.D. Lorenz, "Rotor Position and Velocity Estimation for a Salient-Pole Permanent Magnet Synchronous Machine at Standstill and High Speeds,", *IEEE Tran. Ind. Applicat.*, vol. 34, no. 4, pp. 784-789, July/August 1998.
[66] T. Aihara, A. Toba, T. Yanase, A. Mashimo, and K. Endo, "Sensorless Torque Control of Salient-Pole Synchronous Motor at Zero-Speed Operation," *IEEE Tran. Power Electron*., vol.14, no.1, January 1999, pp. 202-208.
[67] M. Linke, R. Kennel, and J. Holtz, "Sensorless position control of Permanent Magnet Synchronous Machines without Limitation at Zero Speed", *Proc. 2002 IEEE IECON Conf.*, pp. 674-679.
[68] M. Linke, R. Kennel, and J. Holtz, "Sensorless Speed and Position Control of Synchronous Machines using Alternating Carrier Injection", *Proc. 2003 IEEE IEMDC Conf.*, pp. 1211-1217.
[69] J.-H. Jang, S-K. Sul, J.-I. Ha, K. Ide, and M. Sawamura, "Sensorless Drive of Surface-Mounted Permanent-Magnet Motor by High-Frequency Signal Injection Based on Magnetic Saliency,", *IEEE Tran. Ind. Applicat.*, vol. 39, no. 4, pp. 1031-1039, July/August 2003.
[70] J.-I. Ha, K. Ide, T. Sawa, and S.-K. Sul, "Sensorless Rotor Position Estimation of an Interior Permanent-Magnet Motor From Initial States,", *IEEE Tran. Ind. Applicat.*, vol. 39, no. 3, pp. 761-767, May/June 2003.
[71] J.-H. Jang, J.-I. Ha, M. Ohto, K. Ide, and S-K. Sul, "Analysis of Permanent-Magnet Machine for Sensorless Control Based on High-Frequency Signal Injection,", *IEEE Tran. Ind. Applicat.*, vol. 40, no. 6, pp. 1595-1604, November/December 2004.
[72] S. Morimoto, M. Sanada and Y. Takeda, "Mechanical Sensorless Drives of IPMSM With Online Parameter Identification,", *IEEE Tran. Ind. Applicat.*, vol. 42, no. 5, pp. 1241-1248, September/October 2006.
[73] H. Holtz, "Acquisition of Position Error and Magnet Polarity for Sensorless Control of PM Synchronous Machines,", *IEEE Tran. Ind. Applicat.*, vol. 44, no. 4, pp. 1172-1180, July/August 2008.
[74] C.-H. Choi and J.-K. Seok, "Pulsating Signal Injection-Based Axis Switching Sensorless Control of Surface-Mounted Permanent-Magnet Motors for Minimal Zero-Current Clamping Effects,", *IEEE Tran. Ind. Applicat.*, vol. 44, no. 6, pp. 1741-1748, January/February 2008.
[75] S.-C. Yang and R.D. Lorenz, "Surface Permanent Magnet Synchronous Machine Position Estimation at Low Speed Using Eddy-Current-Reflected Asymmetric Resistance,", *IEEE Tran. Power Electron.*, vol. 27, no. 5, pp. 2595-2604, May 2012.
[76] S.-C. Yang and R.D. Lorenz, "Comparison of Resistance-Based and Inductance-Based Self-Sensing Controls for Surface Permanent-Magnet Machines Using High-Frequency Signal Injection,", *IEEE Tran. Ind. Applicat.*, vol. 48, no. 3, pp. 977-985, May/June 2012.
[77] D.D. Reigosa, P. Garcia, F. Briz, D. Raca, and R.D. Lorenz, "Modeling and Adaptive Decoupling of High-Frequency Resistance and Temperature Effects in Carrier-Based Sensorless Control of PM

Synchronous Machines,", *IEEE Tran. Ind. Applicat.*, vol. 46, no. 1, pp. 139-148, January/February 2010.
[78] J.M. Guerrero, M. Leetmaa, F. Briz, A. Zamarron, and R.D. Lorenz, "Inverter Nonlinearity Effects in High-Frequency Signal-Injection-Based Sensorless Control Methods,", *IEEE Tran. Ind. Applicat.*, vol. 41, no. 2, pp. 618-626, March/April 2005.
[79] P. Garcia, F. Briz, M.W. Degner, and D.D. Reigosa, "Accuracy, Bandwidth, and Stability Limits of Carrier-Signal-Injection-Based Sensorless Control Methods,", *IEEE Tran. Ind. Applicat.*, vol. 43, no. 4, pp. 990-1000, July/August 2007.
[80] D. Raca, P. Garcia, D.D. Reigosa, F. Briz, and R.D. Lorenz, "Carrier-Signal Selection for Sensorless Control of PM Synchronous Machines at Zero and Very Low Speeds,", *IEEE Tran. Ind. Applicat.*, vol. 46, no. 1, pp. 167-178, January/February 2010.
[81] D.D. Reigosa, F. Briz, M.W. Degner, P. Garcia, and J.M. Guerrero, "Temperature Issues in Saliency-Tracking-Based Sensorless Methods for PM Synchronous Machines,", *IEEE Tran. Ind. Applicat.*, vol. 47, no. 3, pp. 1352-1360, May/June 2011.
[82] M. Schroedl, "Detection of the rotor position of a permanent magnet synchronous machine at standstill", *Conf. Rec. ICEM* 1988, pp. 195-197.
[83] M. Schroedl, "Operation of the permanent magnet synchronous machine without a mechanical sensor", *Proc. 1990 IET Power Electronics and Variable-Speed Drives Conf.*, pp. 51-54.
[84] M.Schroed1, "Sensorless control of AC Machines at Low Speed and Standstill based on the "INFORM' Method", *Conf. Rec. IEEE IAS 1996*, pp. 270-277.
[85] E. Robeischl and M. Schroedl, "Optimized INFORM Measurement Sequence for Sensorless PM Synchronous Motor Drives With Respect to Minimum Current Distortion,", *IEEE Tran. Ind. Applicat.*, vol. 40, no. 2, pp. 591-598, March/April 2004.
[86] S. Ogasawara and H. Akagi, "Implementation and Position Control Performance of a Position-Sensorless IPM Motor Drive System Based on Magnetic Saliency,", *IEEE Tran. Ind. Applicat.*, vol. 34, no. 4, pp. 806-812, July/August 1998.
[87] T.M. Wolbank and J. Machl, "A modified PWM scheme in order to obtain spatial information of ac machines without mechanical sensor", in Proc. IEEE APEC 2002, vol.1, pp.310-315.
[88] F.M.L. De Belie, P. Sergeant, and J.A. Melkebeek, "A Sensorless Drive by Applying Test Pulses Without Affecting the Average-Current Samples,", *IEEE Tran. Power Electron.*, vol. 25, no. 4, pp. 875-888, April 2010.
[89] J.-L. Shi, T.-H. Liu, and Y.C. Chang, "Position Control of an Interior Permanent-Magnet Synchronous Motor Without Using a Shaft Position Sensor,", *IEEE Tran. Ind. Electron.*, vol. 54, no. 4, pp. 1989-2000 August 2007.
[90] C.-K. Lin, T.-H. Liu, and C.-H. Lo, "Sensorless interior permanent magnet synchronous motor drive system with a wide adjustable speed range,", *IET Electric Power Applicat.*, vol. 3, iss. 2, pp.133-146, 2009.
[91] M. Tursini, R. Petrella, and F. Parasiliti,"Initial Rotor Position Estimation Method for PM Motors", *IEEE Tran. Ind. Applicat.,* vol.39., no.6, November/December 2003, pp. 1630-1640.
[92] M. Boussak, "Implementation and Experimental Investigation of Sensorless Speed Control With Initial Rotor Position Estimation for Interior Permanent Magnet Synchronous Motor Drive,", *IEEE Tran. Power Electron.*, vol. 20, no. 6, pp. 1413-1422, November 2005.
[93] Y. Yan, J.G. Zhu, and Y.G. Guo, "Initial rotor position estimation and sensorless direct torque control of surface-mounted permanent magnet synchronous motors considering saturation saliency,", *IET Electric Power Applicat.*, vol. 2, iss. 1, pp.42-48, 2008.
[94] H.W. De Kock, M. Kaamper, and R. Kennel, "Anisotropy Comparison of Reluctance and PM Synchronous Machines for Position Sensorless Control Using HF Carrier Injection," *IEEE Tran. Power Electron*., vol.24, no.8, August 2009, pp. 1905-1913.
[95] S.-C. Yang, T. Suzuki, R.D. Lorenz, and T.M. Jahns, "Surface-Permanent-Magnet Synchronous Machine Design for Saliency-Tracking Self-Sensing Position Estimation at Zero and Low Speeds,", *IEEE Tran. Ind. Applicat.*, vol. 47, no. 5, pp. 2103-2115, September/October 2011.
[96] A. Faggion, E. Fornasiero, N. Bianchi, and S. Bolognani, "Sensorless capability of fractional-slot surface-mounted PM motors," *Proc. of IEMDC Conf.,* 2011*,* pp.593-598.
[97] N. Bianchi, S. Bolognani, A. Faggion, E. Fornasiero, and A. Sartorello, "Zero-speed sensorless drive capability of fractional-slot inset PM machine," Proc. of IET Power Electronics, Machines and Drives Conf (PEMD), pp.1-6.
[98] J.X. Shen, and K.J. Tseng, "Analyses and Compensation of Rotor Position Detection Error in Sensorless PM Brushless DC Motor Drives,", *IEEE Tran. Energy Conv.* , vol. 18, no.1, pp. 87-93, March 2003.
[99] D.D. Reigosa, P. Garcia, D. Raca, F. Briz, and R.D. Lorenz, "Measurement and Adaptive Decoupling of Cross-Saturation Effects and Secondary Saliencies in Sensorless Controlled IPM Synchronous Machines,", *IEEE Tran. Ind. Applicat.*, vol. 44, no. 6, pp. 1758-1767, November/December 2008.
[100] B. Stumberger, G. Stumberger, D. Dolinar, A. Hamler, and M. Trlep, "Evaluation of saturation and cross magnetization effects in interior permanent-magnet synchronous motor," *IEEE Trans. Industry Applications*, vol. 39, no. 5, 2003.
[101] N. Imai, S. Morimoto, M. Sanada, and Y. Takeda, "Influence of Rotor Configuration on Sensorless Control of Permanent-Magnet Synchronous Motors,", *IEEE Tran. Ind. Applicat.*, vol. 44, no. 1, pp. 93-100, January/February 2008.
[102] R. Wrobel, A.S. Budded, D. Holliday, P.H. Mellor, and P. Sangha, "Design Considerations for Permanent Magnet Brushless Machines for Zero-Speed Sensorless Position Estimation," *Proc. of IEEE IAS Conf.* 2006. vol. 3, pp. 1494 -1500.
[103] P. Sergeant, F. De Belie, and J. Melkebeek, "Effect of Rotor Geometry and Magnetic Saturation in Sensorless Control of PM Synchronous Machines,", *IEEE Tran. Magn.*, vol. 45, no. 3, pp. 1756-1759, March 2009.
[104] Y.Kano, T. Kosaka, N. Matsui, and M. Fujitsuna, "Sensorless-oriented design of concentrated-winding IPM motors for HEV drive application, *Proc. of ICEM Conf.* , 2012, pp.2709-2715
[105] Y.Kano, T. Kosaka, N. Matsui, and T. Nakanishi, "Sensorless-oriented design of IPM motors for general industrial applications," *Proc. of ICEM Conf.*, 2008, pp.1-6.
[106] Y.Kano, T. Kosaka, N. Matsui, and T. Nakanishi, "Design and experimental verification of a sensorless-oriented concentrated-winding IPMSM,", *Proc. of ICEM Conf.*, 2010, pp.1-6.
[107] W. Shanshan, D.D. Reigosa, Y. Shibukawa, M.A. Leetmaa, R.D. Lorenz, and L. Yongdong, "Interior permanent magnet synchronous motor design for improving self-sensing performance at very low speed," Proc. of ICEMS Conf. 2008, pp. 3278 -3283.
[108] K. Akatsu, M.H. Harke, and R.D. Lorenz, "SPMSM Design Considerations for Initial Position and Magnet Polarity Estimation using Carrier Signal Injection," Proc. of IEEE IAS Conf. , 2007, pp. 2393-2398.
[109] J. Bottomley, C. Gerada, and M Sumner, "Electrical machine design for optimal self-sensing properties of SPMSMs,", *Proc. of Power Electronics, Machines and Drives (PEMD)Conf.*, 2012*,* pp.1-5.
[110] D. Reigosa, K. Akatsu, N. Limsuwan, Y. Shibukawa, and R.D. Lorenz, "Self-sensing Comparison of Fractional Slot Pitch Winding vs. Distributed Winding for FW- and FI-IPMSMs Based On Carrier Signal Injection at Very Low Speed,", *Proc. of IEEE ECCE Conf.* , 2009, pp. 3806 -3813
[111] N. Bianchi, D. Durello, and E. Fornasiero, "Multi-objective optimization of a pm assisted synchronous reluctance machine, including torque and sensorless detection capability", Proc. of Power Electronics, Machines and Drives (PEMD) Conf., 2012, pp. 1-6.
[112] N. Bianchi, D. Durello, and E. Fornasiero, "Multi-objective optimization of an interior pm motor for a high-performance drive", Proc. of ICEM Conf., 2012, pp. 376-382.
[113] F. Cupertino, A. Guagnano, A. Altomare, and G. Pellegrino,"Position estimation delays in signal injection-based sensorless PMSM drives", Proc. of IEEE SLED 2012 Symposium, pp.1-6.

VIII. BIOGRAPHIES

Iustin Radu Bojoi (SM'10) received the M.Sc. degree in Electrical Engineering from the Technical University "Gh. Asachi" Iasi, Romania, in 1993, and the Ph.D. degree from Politecnico di Torino, Italy, in 2003. He is currently an Associate Professor in Electrical drives and Power

Electronics. His scientific interests regard the design and development of digital control systems in the fields of power electronics, electrical drives and power-conditioning systems.

Michele Pastorelli was born in Novara, Italy, in 1962. He received his PhD degree in Electrical Engineering from the Politecnico di Torino, Italy, in 1992. He is full professor of electrical machine and drives at the Energy Department of Politecnico di Torino. His mayor fields of interests are high performance control of electric drives (synchronous motors) and the energetic behavior of electric machines and magnetic materials.

Jack Bottomley completed his MEng in electrical engineering at the University of Nottingham in 2009. He has continued to study with the PEMC group at the University of Nottingham, working towards completing a PhD in self-sensing PM machine design in 2013.

Paolo Giangrande was born in Monopoli, Italy, in March 1982. He received his PhD in electrical engineering at the Technical University of Bari in 2011. During 2008 he was a Marie Curie Intra-European Fellow at the University of Malta. Since January 2012, he is research associate at the University of Nottingham within the PEMC group. His research interests include sensorless control of AC electric drives and intelligent motion control, as well as modelling and parameters identification of electrical machine for aerospace application.

Chris Gerada received his PhD in numerical modeling of high performance electrical machines at the University of Nottingham in 2005 within the PEMC group. He was then appointed as a postdoctoral researcher, Lecturer in 2008 and Associate Professor in 2011. His principal research interests lie in high performance electrical machines and drives. He was awarded a Royal Academy of Engineering Senior Research Fellowship and is an associate editor of the IEEE IAS transactions.